Functional Materials 18, No.1 (2011)

HCP and FCC phases in Ni–Pd laser thin films

A.G.Bagmut, I.G.Shipkova, V.A.Zhuchkov

National Technical University "Kharkiv Polytechnical Institute",
21 Frunze Str., 61002 Kharkiv, Ukraine

Received April 16, 2010

Using transmission electron microscopy, electron diffraction, and vibrating sample magnetometry techniques, studied have been the films of Pd, Ni, and a Ni–Pd alloy deposited by pulsed laser ablation both of single-element and composite two-element Ni–Pd targets. It was established that at alternate deposition of laser erosion Ni and Pd plasma, films with metastable hexagonal (hcp) crystal lattice can be formed. Crystallographic parameters of this lattice grow monotonically with increasing Pd content. After annealing, these films take the equilibrium cubic (fcc) structure and transform to ferromagnetic state. The dependence of the solid solution lattice constant of Ni–Pd alloy on the Pd concentration exhibits a positive deviation from the Vegard's law.

Методами просвечивающей электронной микроскопии, электронографии и вибрационной магнитометрии исследованы пленки Ni и сплавов Ni–Pd, осажденные импульсным лазерным распылением как одноэлементных, так и составных двухэлементных мишеней Ni–Pd. Установлено, что при попеременном осаждении лазерной эрозионной плазмы Ni и Pd на подложках могут формироваться пленки с метастабильной кристаллической решеткой ГПУ, параметры которой монотонно возрастают с увеличением содержания Pd. После отжига пленки приобретают равновесную структуру ГЦК и переходят в ферромагнитное состояние. Наблюдается положительное отклонение от закона Вегарда зависимости постоянной решетки твердого раствора сплава Ni–Pd от концентрации Pd.

1. Introduction

In bulk state, Ni, Pd and alloys of Ni–Pd system which is characterized by the complete mutual solubility of components in both solid and liquid states have face-centered cubic (fcc) crystal lattice [1]. While hexagonal close-packed (hcp) structure (α-Ni phase) along with equilibrium fcc structure (β-Ni phase) is possible in thin film and nanocrystalline states. The α-Ni phase has been observed at electron diffraction patterns research of Ni films deposited by thermal evaporation in vacuum. An interpretation of hcp Ni formation based on the phase size effect has been proposed [2]. This effect is associated with the free energy change of the film-substrate system at increasing relative fraction of surface when the film thickness decreases. The crystallographic parameters of α-Ni and β-Ni phases according to the tables of International Center for Diffraction Data — JCPDC are cited in [3, 4].

In recent years, the interest in the Ni films and nanoparticles as well as Ni–Pd ones rises sharply. It is due to their magnetic, electrophysical, and catalytic properties. Moreover, the Ni–Pd alloys are very promising for medical purposes as the materials for self-controlled hyperthermia [5]. Ni nanoparticles of both hcp and fcc phases have been obtained by chemical synthesis [6]. The preparation of Ni nanoparticles having nonequilibrium hcp lattice by sol-gel method was described in [7]. The sol (the solution of $Ni(NO_3)_2$ and $C_6H_8O_6$) was heated to form gel. The latter was used as a precursor for synthesis of Ni particles at heat-treatment in argon atmosphere. The powders consisting of Ni particles of hcp structure only or fcc one as well as a mix-

ture of two types of particles were obtained depending on heat-treatment temperature.

The data concerning to magnetic properties of α-Ni nanoparticles are ambiguous. According to [6], the nanoparticles of diameter D ranging from 8.5 to 18 nm show antiferromagnetic behavior while β-Ni nanoparticles of 11–26 nm diameters reveal ferromagnetic properties. In a number of works, there are the data that α-Ni nanoparticles may be in nonmagnetic, antiferromagnetic, and ferromagnetic states [8].

The island Ni films with hcp crystal lattice have been obtained during heteroepitaxial growth of Ni onto (001) MgO surface at the substrate temperature T_s = 390 K [5]. However, the transformation of hcp lattice to fcc one occurred by martensite mechanism when the island lateral size increased (above ~5 nm). The formation of Ni islands having unstable hcp lattice was explained in by pseudomorphism. According to this phenomenon, at an initial stage of growth the crystalline lattice of film was arranged to that of substrate.

Today, the formation of metastable hcp phase in Ni films is a well-established fact [10]. Continuous films of both α-Ni and β-Ni were obtained by pulsed plasma evaporation technique in [10, 11]. Only the β-Ni films have revealed ferromagnetic properties. The α-Ni films and hcp films of α-Ni_3N phase which was formed in nitrogen atmosphere of 10^{-2} Torr had no ferromagnetic properties [11].

A specific feature of pulsed laser deposition (PLD) method consists in the discrete delivery of periodic flux of laser erosion plasma comprising electron, ion and neutral components to substrate. The nucleation and growth of clusters on the substrate proceeds in nonequilibrium conditions predetermining the formation possibility of metastable structural states. That method was used to obtain the continuous Ni films of a metastable hcp structure [12–17]. The volume changes [14] and orientational relations [15] between crystalline lattices were established in the course of the hcp-fcc transition at annealing. It was confirmed that only fcc Ni films possess the ferromagnetic properties.

According to [17], the formation of hcp phase is possible not only in Ni films but also in Ni–Pd alloy ones if the PLD method is used. The aim of this work is to obtain and to investigate the structure, phase composition and magnetic characteristics of films deposited by laser sputtering of combined targets of Ni and Pd.

2. Techniques

The films were deposited in vacuum onto the (001) KCl substrates disposed on the path of vapour plasma flux. The flux was formed by sputtering of target using pulses of an LTI PCh-5 optical quantum generator operating in a Q-switched mode. The laser wavelength and the pulse repetition rate were 1.06 μm and 25 Hz, respectively. During deposition, the residual gas pressure in vacuum chamber was 10^{-5} Torr. The substrate temperature T_s was about 440–450 K.

The rotating disks consisting of sectors made of high-purity Ni and Pd were used as targets subjected to sputtering. The rotation frequency was 55–85 s^{-1}. This technique allowed us to deposit laser erosion plasma of Ni or Pd onto substrate alternately. The ratio $C_M = S_{Pd}/S_0$ of the area scanned by the laser beam over the palladium surface S_{Pd} to the total disk surface area S_0 was varied between 0, 0.25, 0.5, 0.75 and 1. This way allowed us to obtain both single-element films of Ni ($C_M = 0$) or Pd ($C_M = 1$) and the films of Ni–Pd alloys. The film thickness was about 28–30 nm. Structure and phase transformations were initiated by annealing of the films in vacuum without separation from substrates. The temperature T_0 and annealing period τ_0 were 710–720 K and 3 h, respectively.

The films were separated from substrates in distilled water and transferred onto copper grids for electron microscopic investigations. The structure was studied by electron diffraction and transmission electron microscopy using PEM-100-01 and EM-100L electron microscopes. The scale of the electron diffraction patterns was estimated by the traditional technique using calibration thin film of polycrystalline Al. Basing on bright field electron micrographs of the films, the mean values of grain sizes D were determined prior to and after the annealing.

The magnetic properties of the films in as-deposited state and after annealing were studied using a high sensitive vibrating sample magnetometer. Hysteresis loops were measured at room temperature for the samples of square shape with an area of ~1 cm^2 in magnetic fields up to 1000 Oe applied at two mutually perpendicular directions in the film plane. The mean saturation magnetization I_S were determined by comparing signals of the reference sample and tested one of known area and thickness.

3. Results and discussion

Fig.1a shows the electron diffraction pattern, its scheme and the electron micrograph of the film deposited at substrate temperature T_s = 440 K by pulse laser sputtering of Ni target (C_M = 0). The film is polycrystalline, the mean grain size $\overline{D}$ amounts 5.9 nm. The experimental electron diffraction pattern (see left upper part of the Figure) is combined with theoretical one (see left bottom part of Figure) for the polycrystal of hcp structure. The circle radii of the theoretical electron diffraction pattern satisfy the equation:

$$R = G\sqrt{\frac{4}{3}(h^2 + hk + k^2) + \frac{3}{8}l^2}. \qquad (1)$$

It is taken into account in the Eq. 1 that for hcp structure the ratio of parameters of crystal lattice unit cell $G = c/a = \sqrt{8/3}$, G is the scale factor, h, k, l are the Miller's indices for crystal planes. For hcp structure, the reflexes with odd value of $(4h + 2k+3l)/3$ are forbidden. Therefore, the circles with diameters satisfying to such equation do not show in the theoretical electron diffraction pattern. If the experimental electron diffraction pattern corresponds to that of hcp film, it is possible to obtain complete coincidence of the rings of the experimental electron diffraction pattern with the circles of the theoretical one by changing the scale factor G. Since this is observed for experimental electron diffraction pattern shown in Fig.1a, we have attributed to the reflexes numbered as 1, 2, 3 and so on the h, k, l indices of hcp lattice.

The interpretation of the electron diffraction pattern shown in Fig.1a evidences that the metastable α-Ni phase with parameters $\boldsymbol{a}$ = 0.265±0.001 nm, $\boldsymbol{c}$ = 0.432±0.001 nm and γ = 1.63±0.01 is formed during laser deposition of Ni onto KCl substrate at T_s = 440 K. These values are close to data from [6, 7] obtained by X-ray diffraction analysis of hcp Ni nanoparticles.

As a result of annealing (τ_0 = 3 h, T_0 = 710 K) the crystalline lattice of Ni films is transformed. The electron diffraction pattern, its scheme, and the electron micrograph are shown in Fig.1b. After annealing, a low ordering of Ni layer arises in parallel orientation relative to (001) KCl substrate. The mean grain size $\overline{D}$ of Ni increased to 62.7 nm after annealing. The circle radii of the theoretical electron diffraction pattern of fcc polycrystal satisfy the equation:

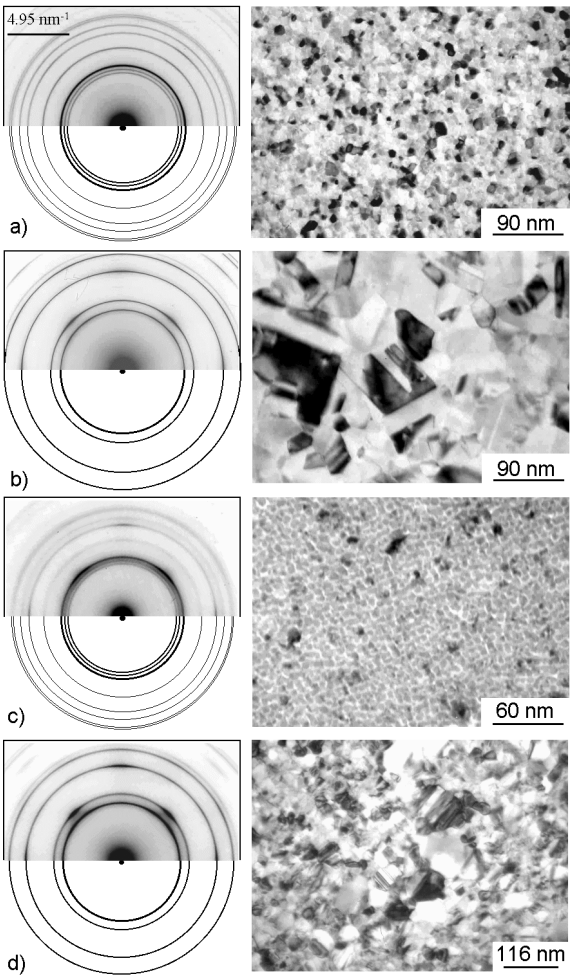

Fig.1. Electron diffraction patterns with schemes and electron micrographs of structure of the films deposited at T_s = 440 K by pulse laser sputtering. (a) Sputtering of Ni (C_M = 0), as-prepared state. (b) The same after annealing of the film. (c) Sputtering of composite 0.5Ni–0.5Pd target (C_M = 0.5), as-prepared state. (d) The same after annealing of the film. The electron diffraction pattern contrast is inverted.

$$R = G\sqrt{(h^2 + k^2 + l^2)}\ , \qquad (2)$$

the reflexes of the same evenness being allowed for fcc structures. Since in Fig.1b the rings of the experimental electron diffraction pattern coincide with the circles of the theoretical electron diffraction pattern for fcc structure, we have to attribute the h, k, l reflection indices to fcc lattice. After annealing the film acquires the fcc structure with the lattice parameter a_0 = 0.352±0.001 nm.

As the result of the sputtering of composite 0.75Ni–0.25Pd (C_M = 0.25) target

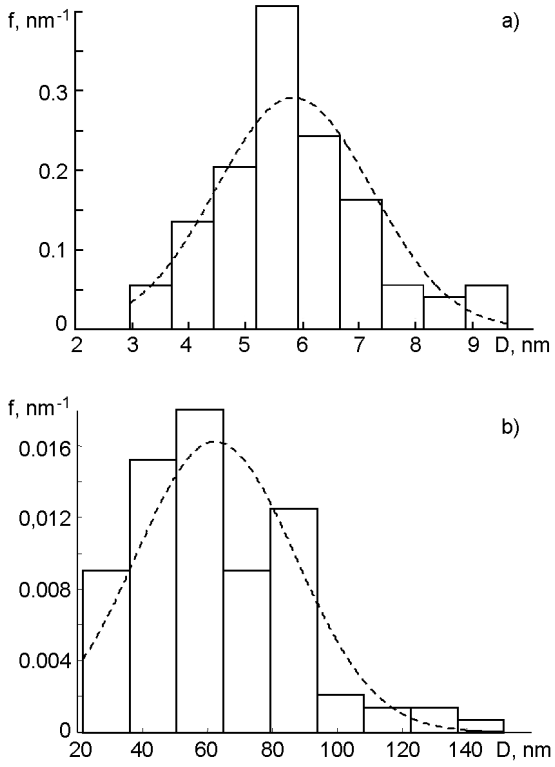

Fig.2. Histograms of grain size distribution in the films obtained by pulse laser deposition. (a) Sputtering of Ni ($C_M = 0$), as-prepared state. (b) The same after annealing of the film. D is the grain size, f is the frequency function. Dotted curve corresponds to probability density of normal distribution of D.

and 0.5Ni–0.5Pd ($C_M = 0.5$) one, the Ni–Pd alloy films are formed onto substrates. Their crystal lattices corresponded to hcp structure, too. In Fig.1c, the electron diffraction pattern, its scheme, and the electron micrograph of the film deposited at substrate temperature $T_s = 440$ K using laser sputtering of composite 0.5Ni–0.5Pd target are shown. The film is polycrystalline with the mean grain size $\overline{D} = 5.4$ nm. The formation of Ni–Pd alloy film with metastable hcp crystal lattice takes place. The film parameters are as follows: $a = 0.273 \pm 0.001$ nm, $c = 0.451 \pm 0.001$ nm and $\gamma = 1.65 \pm 0.01$. As a result of the annealing, the film crystal lattice is transformed to fcc structure with parameter $a_0 = 0.374 \pm 0.001$ nm. The value increases up to 36.3 nm.

Fig.2 shows the histograms which characterize the distribution of D measuring data in as-prepared films and annealed ones. On the all diagrams, the values of f corresponding to relative frequency density of D values are exposed on the ordinate axis. By definition:

$$f = \frac{n_i}{N\Delta D}, \tag{3}$$

where n_i is the frequency of values of D lying in the i-th interval, ΔD is the width of the interval, N is the total number of measurements. For reference, the broken curves corresponding to normal distribution probability density f_n are shown on the plots:

$$f_n = \frac{1}{\sigma\sqrt{2\pi}} \exp\left(-\frac{(D - \overline{D})^2}{2\sigma^2}\right), \tag{4}$$

where σ is the standard deviation of D (σ is equal to 1.4 and 24.6 nm for Fig.2a and 2b, respectively). Comparing the f_n curve and the arrangement of histogram columns evidences that the distribution of grain sizes is similar to the normal one.

The films with hcp lattice are formed onto (001) KCl substrate at $T_s = 440$ K at the sputtering of Ni, 0.75Ni–0.25Pd, and 0.5Ni–0.5Pd targets. However, at 0.25Ni–0.75Pd target sputtering ($C_M = 0.75$) the films of both hcp and fcc phase are formed. For hcp phase, $a = 0.276 \pm 0.001$ nm, $c = 0.452 \pm 0.001$ nm and $\gamma = 1.64 \pm 0.01$. For fcc one, $a_0 = 0.380$ nm. Parameter γ is close to theoretical value for close-packed structure, viz. to $(8/3)^{1/2} = 1.633$. At the same time, the parameters of hcp structure (a and c) increase monotonically when palladium content in the film increases (C_M increase from 0 to 0.75). This fact is illustrated in Fig.3 for the parameter a. The straight line, plotted according to the least-squares method, is a regression line of the parameter a of hcp cell on C_M. The correlation coefficient describing a tightness of linear connection between C_M and a values is close to 1 in this case.

In all cases, the film after annealing gains the fcc structure. Under assumption that C_M coincides with the molar concentration of Pd in the film, our experimental data agree satisfactorily with data from other authors for Ni–Pd alloys in bulk state [1]. In Fig.3b the dependence of the constant a_0 versus C_M for the solid solution having intermediate content is shown. The solid curve is the result of fitting of experimental points by least-squares method using the polynomial of degree 3. In accordance with Vegard law [18], in the simplest case, the a_0 value depends linearly on molar concentration of one of the components. For comparison, in Fig.3b the broken curve is plotted using the equation:

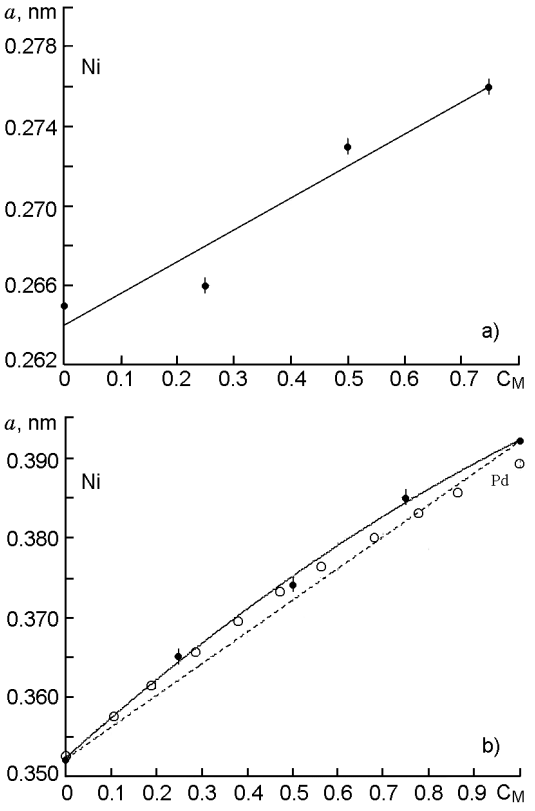

Fig.3. Dependence of the lattice parameters of Ni–Pd solid solution on the sputtered target composition. (a) Dependence of the parameter a for hcp cell vs Pd content in sputtered target. (b) Dependence of the lattice parameter a_0 of Ni–Pd solid solution vs sputtered target composition (solid line). Dotted straight line is drawn according to Vegard law using relation (5). • — Electron diffraction data of thin film state measuring in present work. ° — Data concerning to bulk Ni–Pd system [1].

$$a_0 = a_0(\mathrm{Ni}) \cdot (1 - C_M) + a_0(\mathrm{Pd}) \cdot C_M, \quad (5)$$

where a_0(Ni) and a_0(Pd) are the lattice parameters of pure Ni and Pd components, respectively. A comparison between line 1 and line 2 evidences positive deviation of the $a_0(C_M)$ dependence from Vegard law, since curve *2* joining the experimental points of lattice parameter values lies above line *3*. The positive deviation from Vegard law is typical of the alloys with concave liquidus in phase diagram that is the case for Ni–Pd system [19]. At the same time, a linear dependence of lattice parameters of solid solution (both a and c) versus C_M (see straight line in Fig.3a) presupposes that Vegard law is realized within a limited interval of Pd

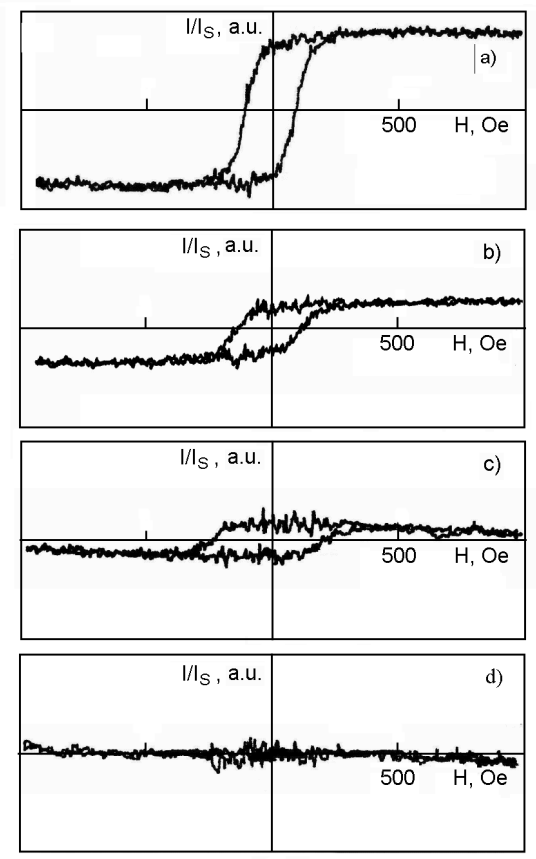

Fig.4. Magnetization curves of the films obtained by pulse laser deposition and those annealed on substrate. (a) Sputtering of Ni ($C_M = 0$). (b) Sputtering of composite 0.75Ni–0.25Pd target ($C_M = 0.25$). (c) Sputtering of composite 0.5Ni–0.5Pd target ($C_M = 0.5$). (d) Sputtering of composite 0.25Ni–0.75Pd target ($C_M = 0.75$).

concentrations where the films before annealing had hcp crystalline lattice.

The measurements of magnetic characteristics has shown that Ni and Ni–Pd alloy films with metastable hcp structure magnetized in the fields up to 1000 Oe did not exhibit magnetic moment above the sensitivity threshold of magnetometer used. This sensitivity threshold for above mentioned sizes of the samples under study corresponds to magnetization values not exceeding 1–5 G. After the annealing that initiated the hcp→fcc phase transformation, the magnetic state of Ni–Pd films with $C_M = 0$–0.5 changed sharply. The magnetic moment increased considerably and the hysteresis is observed at magnetization reversal (see Fig.4a, 4b, 4c). The in-plane anisotropy was absent. For Ni films, the coercive force $H_C \approx 120$ Oe, the saturation field $H_S \approx 250$ Oe.

The similar data for 0.75Ni–0.25Pd films were H_C≈130 Oe, H_S≈500 Oe (Fig.4b). For 0.5Ni–0.5Pd films, H_C was 210 Oe and H_S was 500 Oe. Similar changes of magnetic moments of Ni films after annealing accompanied by structure transformation from hcp to fcc lattice have been observed in [13, 15–17]. The films with a high Pd concentration (C_M≥0.75) did not possessed magnetic moment neither before nor after the annealing (Fig.4d). It shout be noted that in bulk state at room temperature the range of ferromagnetic alloys [1] is limited with the same concentration range as in examined Ni–Pd films after annealing.

4. Summary

It was established that pulse laser deposition method makes it possible to obtain not only the Ni films of metastable hcp structure but also Ni–Pd alloy films in the course of alternating sputtering of the Ni and Pd components of composite target. The hcp lattice parameters (a and c) of Ni–Pd alloy films increase monotonically with increasing palladium content in sputtered target from 0 to 75 %. At the same time, the ratio c/a is close to the theoretical value 1.63 within the experimental error. As a result of the annealing, the Ni and Ni–Pd alloy films acquire the equilibrium fcc structure. A positive deviation of the dependence of solid-solution lattice constant on Pd content from Vegard law takes place. In as-prepared state, Ni and Ni–Pd alloy films with the hcp structure are characterized by absence of magnetic moment. After annealing, the transition to ferromagnetic state occurs, the hysteresis is observed at magnetization reversal.

References

1. O.M.Barabash, Yu.N.Koval, Structure and Properties of Metals and Alloys. A Reference Book, Naukova Dumka, Kyiv (1986) [in Russian].
2. A.I.Bublik, B.Ya.Pines, *Dokl. Akad. Nauk SSSR*, **87**, 215 (1952).
3. International Centre for Diffraction Data – JCPDC, 1996, card No.45-1027.
4. International Centre for Diffraction Data – JCPDC, 1996, card No.04-0850.
5. J.G.Meijer, N.van Wieringen et al., *Med. Phys.*, **22**, 101 (1995).
6. Yoon Tae Jeon, Je Yong Moon, Gang Ho Lee et al., *J. Phys. Chem. B*, **110**, 1187 (2006).
7. L.L.Gong, Y.Liu Wang, J.H.Yang et al., *J. Alloys and Comp.*, **457**, 6 (2008).
8. Yuanzhi Chen, Dong-Liang Peng, Dongxing Lin et al., *Nanotechnolology*, **18**, 1 (2007).
9. W.Tian, H.P.Sun, X.Q.Pan et al., *Appl. Phys. Lett.*, **86**, 131915 (2005).
10. S.M.Zharkov, V.S.Zhigalov, G.I.Frolov, *Fiz. Metal. Metalloved.*, **81**, 170 (1996).
11. V.S.Zhigalov, G.I.Frolov, V.G.Myagkov, *Zh. Tekhn. Fiz.*, **68**, 136 (1998).
12. J.Vergara, V.Madurga, *J. Mater. Res.*, **17**, 8 (2002).
13. A.G.Bagmut, I.G.Shipkova, V.A.Zhuchkov, *Functional Materials*, **16**, 161 (2009).
14. A.G.Bagmut, V.A.Zhuchkov, I.G.Shipkova et al., *Poverkhnost: X-ray, Synchrotronous, and Neurton Res.*, No.10, 54 (2009).
15. A.G.Bagmut, I.G.Shipkova, V.A.Zhuchkov, *Metallofiz. Noveysh. Technologii*, **31**, 827 (2009).
16. A.G.Bagmut, I.G.Shipkova, V.A.Zhuchkov, *Functional Materials*, **16**, 405 (2009).
17. A.G.Bagmut, I.G.Shipkova, V.A.Zhuchkov, *Pis'ma Zh. Tekhn. Fiz.*, **36**, 52 (2010).
18. L.Vegard, *Zeitschrift fur Physik*, **5**, 17 (1921).
19. G.B.Bokiy, Crystal Chemistry. MGU Publ., Moscow (1960) [in Russian].

ГЩП та ГЦК фази у тонкоплівкових лазерних конденсатах Ni–Pd

О.Г.Багмут, І.Г.Шипкова, В.А.Жучков

Методами просвічуваної електронної мікроскопії, електронографії та вібраційної магнітометрії досліджено плівки Ni та сплавів Ni–Pd, осаджені імпульсним лазерним розпилюванням як одноелементних, так і компонованих двоелементних мішеней Ni–Pd. Установлено, що при поперемінному осадженні лазерної ерозійної плазми Ni та Pd на підкладках можуть формуватися плівки з метастабільною кристаллічною решіткою ГЩП, параметри якої монотонно зростають зі збільшенням вмісту Pd. Після відпалу плівки отримують рівноважну структуру ГЦК і переходять у феромагнітний стан. Спостерігається позитивне відхилення від закону Вегарда залежності сталої решітки твердого розчину сплаву Ni–Pd від концентрації Pd.